

## Ion Solvation in a Water–Urea Mixture

Takeshi Yamazaki,<sup>†</sup> Andriy Kovalenko,<sup>\*,†,§</sup> Vladimir V. Murashov,<sup>‡,||</sup> and Grenfell N. Patey<sup>‡</sup>

National Institute for Nanotechnology, 11421 Saskatchewan Drive, Edmonton, Alberta, T6G 2M9, Canada and  
Department of Chemistry, University of British Columbia, Vancouver, British Columbia V6T 1Z1, Canada

Received: September 11, 2009; Revised Manuscript Received: October 22, 2009

We employ molecular dynamics simulations and the reference interaction site model (RISM) integral equation theory to study the solvation structure and solvation thermodynamics of the transfer process from water to a water–urea mixture. Simple positive and negative ions together with uncharged species of the same size are used as crude models for the hydrophilic and hydrophobic groups of a protein. We find that urea preferentially solvates positively charged species. The solvation free energies obtained indicate that larger solutes favor the transfer from water to a water–urea mixture. The decomposition of the transfer free energy into the energetic and entropic terms shows that the energetic part is much larger than the entropic one and tends to dominate the transfer process, supporting the direct mechanism of urea-denaturation. In addition, the effect of urea on the water liquid structure is discussed from the viewpoint of solvation entropy.

### Introduction

In many in vitro folding and unfolding experiments, urea is used as a well-established denaturant. The ability of urea to denature the native structure of globular proteins is well-known; however, the mechanism of urea denaturation is not fully understood. Despite extensive experimental and theoretical studies, a satisfactory explanation of the mechanism of urea denaturation has been difficult to find because of the complexities of urea interaction with water and proteins. There are two views proposed for the mechanism of urea denaturation: (1) Based on the observation that the solubilities of hydrophobic side chains of peptides increase in water–urea mixtures, it is proposed that protein denaturation is due to changes in the hydrophobic effect. That is, the solvation of hydrophobic species is thought to be the driving force of protein denaturation. (2) The urea molecules directly interact with the peptides. At a certain critical number of hydrogen bonds between urea molecules and the protein, the unfolded state becomes more stable. Historically, urea denaturation has been described largely in terms of the hydrophobic effect. While recent theoretical studies seem to support the latter mechanism,<sup>1–13</sup> others argue that both mechanisms are equally relevant.<sup>14,15</sup>

To date, most theoretical studies of solvation in water–urea mixtures employed only molecular simulation methods. In this work, we are interested in the change of the solvation free energy of simple ions, and related uncharged species, in transfer from water to a water–urea mixture. To obtain the free energy of the transfer, we utilize the reference interaction site model (RISM) integral equation theory of molecular liquids.<sup>16–19</sup> The RISM theory yields the thermodynamic properties (including energy–entropy decomposition) as well as the microscopic solvation structure with reasonable computational cost. We obtain the solvation structure of solutes in water and in the

water–urea mixture by using the RISM theory as well as molecular dynamics (MD) simulations and compare the results from both the approaches. Given that the RISM theory is much less computationally expensive, it is well worthwhile to evaluate it by comparing with MD results and to analyze the transfer physics from both viewpoints.

To obtain insight into urea denaturation of complex proteins, it would be valuable to elucidate the solvation of individual amino acid fragments or simpler charged and uncharged species. The free energy of association of methane with methane<sup>1,2</sup> and of urea with aromatic hydrocarbons<sup>20</sup> in water–urea mixtures has been investigated by Monte Carlo and MD simulations. The solvation of rare gases and aliphatic hydrocarbons in a water–urea mixture<sup>7,8</sup> has been investigated by MD simulations, and thermodynamic data for nonpolar solute transfer from water to a water–urea mixture have been analyzed by scaled particle theory.<sup>5,6</sup> Here we use simple ions and corresponding uncharged species (obtained by dropping the ionic charges) as models for hydrophilic and hydrophobic groups, respectively. We consider systems in which a simple ion is dissolved in solvent at infinite dilution, such that the correlations among solvent molecules are not changed by the solute. Attention is focused on extracting the simple physics of the transfer from the solute–solvent correlations and on analyzing the transfer solvation free energy in terms of the energetic and entropic parts.

### Methods

**RISM Integral Equation Theory.** Since the transfer free energy of aliphatic hydrocarbons<sup>5</sup> and simple ions<sup>21</sup> from water to water–urea mixture are very subtle quantities, one has to be very careful in choosing a closure relation to complement the RISM integral equations. Among the several closures examined, we found that the Kovalenko–Hirata (KH) approximation<sup>19,22,23</sup> can reasonably reproduce the experimental transfer solvation free energies for the systems in which we are interested (see the Supporting Information for further details). We have also confirmed that the Gaussian fluctuation (GF) approximation proposed by Chandler et al.<sup>24</sup> improves the agreement of the solvation free energy with experiments, as has been pointed out in several studies.<sup>25–28</sup> However, the transfer properties obtained

\* To whom correspondence should be addressed. E-mail: andriy.kovalenko@nrc-cnrc.gc.ca.

<sup>†</sup> National Institute for Nanotechnology.

<sup>‡</sup> University of British Columbia.

<sup>§</sup> Department of Mechanical Engineering, University of Alberta, Edmonton, Canada.

<sup>||</sup> Current address: National Institute for Occupational Safety and Health, Washington, D.C. 20201.

with and without including the GF approximation were almost identical, as has been previously observed,<sup>26</sup> and both methods reasonably reproduce the experimental results. In the present study, we use the KH closure without the GF approximation to simplify the theoretical framework. From the RISM-KH equations, the solvation free energy  $\mu$  of a simple solute is obtained in the closed analytical form

$$\mu = k_B T \sum_v \sum_{\alpha} \rho_{\alpha} \int d\mathbf{r} \left[ \frac{1}{2} h_{\alpha}^2(r) \Theta(-h_{\alpha}(r)) - c_{\alpha}(r) - \frac{1}{2} h_{\alpha}(r) c_{\alpha}(r) \right] \quad (1)$$

where  $k_B T$  is the Boltzmann constant times the temperature of the solution,  $v$  denotes a molecular solvent species,  $\alpha$  denotes an atomic interaction site on solvent species  $v$ , and  $\rho_{\alpha}$  is the number density of site  $\alpha$ .  $c_{\alpha}(r)$  is the direct correlation function between the solute and solvent site  $\alpha$ , and  $h_{\alpha}(r)$  is the corresponding total correlation function related to the radial distribution function  $g_{\alpha}(r) = h_{\alpha}(r) + 1$ .  $\Theta(x)$  is the Heaviside step function switching the term  $(1/2)h_{\alpha}^2(r)$  on and off in the spatial areas of density depletion ( $h_{\alpha}(r) < 0$ ) and enrichment ( $h_{\alpha}(r) > 0$ ), respectively. The solute–solvent total and direct correlation functions,  $h_{\alpha}(r)$  and  $c_{\alpha}(r)$ , are determined by solving the RISM equation for systems in which the solute is solvated at infinite dilution in water or in a water–urea mixture,

$$h_{\alpha}(r) = \sum_{\gamma} \int d\mathbf{r}' c_{\gamma}(|\mathbf{r} - \mathbf{r}'|) \{ \omega_{\gamma\alpha}^{\text{vv}}(r') + \rho_{\gamma} h_{\gamma\alpha}^{\text{vv}}(r') \} \quad (2)$$

complemented with the KH closure,

$$g_{\alpha}(r) = \begin{cases} \exp(d_{\alpha}(r)) & \text{for } d_{\alpha}(r) \leq 0 \\ 1 + d_{\alpha}(r) & \text{for } d_{\alpha}(r) > 0 \end{cases} \quad (3a)$$

$$d_{\alpha}(r) = -u_{\alpha}(r)/(k_B T) + h_{\alpha}(r) - c_{\alpha}(r) \quad (3b)$$

$\omega_{\gamma\alpha}^{\text{vv}}(r)$  is the intramolecular distribution function specifying the geometry of solvent molecules.  $h_{\gamma\alpha}^{\text{vv}}(r)$  is the total correlation function between interaction sites of molecules of solvent, which is obtained in advance by solving the RISM equation for pure solvent.

Under the isochoric condition, the solvation free energy  $\mu$  can be decomposed into the solvation energetic and entropic parts

$$\mu = \varepsilon - TS \quad (4)$$

where  $\varepsilon$  is the solvation energy term and  $-TS$  is the solvation entropy multiplied by the temperature  $T$ . In turn, the solvation energy  $\varepsilon$  can be viewed as consisting of two contributions: one arising from creation of a polarized cavity (in pure solvent), referred to as the reorganization energy  $\varepsilon^{\text{org}}$ , and the other corresponding to the energy of embedding the solute molecule into the cavity, referred to as the average solute–solvent energy  $\varepsilon^{\text{ave}}$ , which is expressed as

$$\varepsilon^{\text{ave}} = \sum_v \sum_{\alpha} \rho_{\alpha} \int d\mathbf{r} u_{\alpha}(r) g_{\alpha}(r) \quad (5)$$

where  $u_{\alpha}(r)$  is the site–site pair potential between the simple spherical solute and solvent site  $\alpha$ . For the site–site pair potentials, we choose the standard model consisting of Lennard–Jones (LJ) and electrostatic interaction terms. For water, we employ the SPC/E model<sup>29</sup> modified by ascribing a LJ size parameter sigma to the hydrogen site to optimize the RISM description of water structure.<sup>30</sup> We use the OPLS force

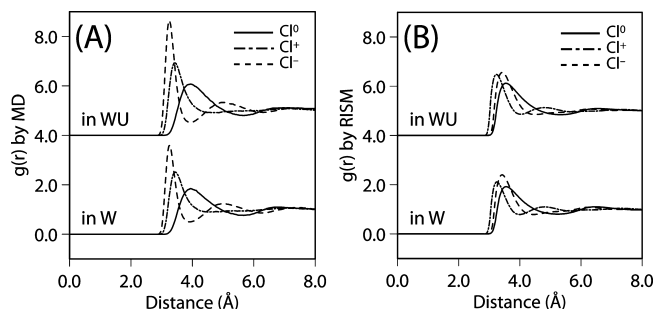


**Figure 1.** Radial distribution functions (RDFs) between the chloride-size solutes and the oxygen atom of water. Uncharged, positive, and negative ions are plotted as solid, dash-dotted, and dashed lines, respectively. Panel A is the RDF obtained by MD simulations, and panel B is that given by RISM theory. In both panels, the RDFs in water and in water–urea (displaced upward by 4.0 units) are plotted.

field for urea<sup>31</sup> and employ the parameters proposed by Koneshan et al.<sup>32</sup> for the ions. We examined the following seven ions: Na, K, Rb, Cs, Cl, Br, I; as well as four fictitious particles with a LJ sigma of 5.5, 6.0, 6.5, and 7.0 Å, while keeping the potential well depth (LJ  $\varepsilon$ ) the same as for the other ions. We used the number density  $0.03333 \text{ Å}^{-3}$  for pure water. In the case of the water–urea mixture, we used the partial number densities  $0.02131$  and  $0.004816 \text{ Å}^{-3}$  for water and urea, respectively, which corresponds to an 8 M water–urea mixture. These number densities are consistent with those used in the molecular dynamics simulations described below. The temperature considered is 300 K. It should be noted that the recent hybrid RISM-SCF calculations predicted that the structure of urea at infinite dilution in water is nonplanar, whereas the OPLS model assumes a planar structure.<sup>33</sup> We calculated the temperature derivative of the solvation free energy, based on the analytical variation of the RISM equation.<sup>34</sup>

**Molecular Dynamics Simulation.** MD simulations were performed on pure water (255 water molecules in a box with side length of  $19.705 \text{ Å}$ ) and a urea–water mixture (208 water molecules plus 47 urea molecules in a box with side length of  $21.37 \text{ Å}$ ). There was one ion (or uncharged species) per box in all calculations. We used the same number densities for solvents as in the case of the RISM calculation. The temperature was maintained at 300 K by velocity scaling every 100 time steps. The LJ parameters and the mass used to describe solute particles were those of the chloride ion. Systems were equilibrated for 0.4 ns. Averages were accumulated for 2.4 ns for urea–water mixtures or 0.4 ns for pure water. In all calculations, cubic cells with periodic boundary conditions were employed and the long-range forces were handled using the Ewald summation method. The equations of motion were integrated using a fourth-order predictor–corrector algorithm<sup>35</sup> with time step  $\Delta t = 4 \text{ fs}$ .

## Results and Discussion

### Solvation Structure: Comparison between MD and RISM.

Figure 1 show the radial distribution functions (RDFs) between the chloride-size solutes (with charges of 0, +1, and –1) and the oxygen atom of water. The RDFs obtained from MD simulations are plotted in Figure 1A, and those given by the RISM theory in Figure 1B. From Figure 1, one notices that the MD and RISM results agree well for the positive ion and for the neutral solute, but that there is some discrepancy for the negative ion. The negative ion peak is shifted inward and is higher in the case of MD than for RISM. This discrepancy is related to the well-known shortcoming of RISM theory with

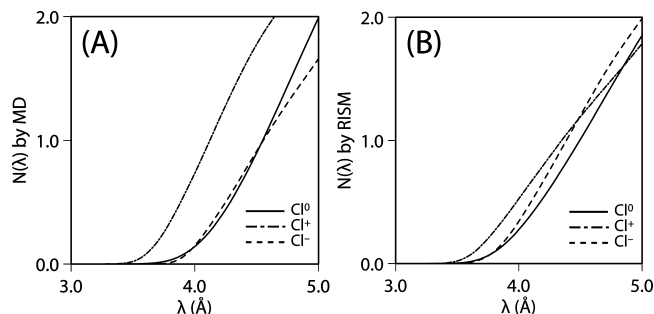


**Figure 2.** Running coordination numbers  $N(\lambda)$  of the urea carbon site around the chloride-size solutes as a function of distance  $\lambda$ . Uncharged, positive, and negative ions are plotted as solid, dash-dotted, and dashed lines, respectively. Panel A is the  $N(\lambda)$  obtained by MD simulations and panel B is that given by the RISM theory.

treatment of auxiliary interaction sites. Water molecules are associated to  $\text{Cl}^-$  directly by hydrogen bonding with their hydrogens, whereas the negatively charged oxygens are found near  $\text{Cl}^-$  mainly because of the O–H intramolecular bonds. These bonds enter the RISM equation only through the intramolecular matrix and are absent in any local, two-body closure approximation. Therefore, the intramolecular bond constraint is not strictly enforced on the positions of the  $\text{Cl}^-$ –H and  $\text{Cl}^-$ –O peaks. The oxygen peak is more loosely coordinated to  $\text{Cl}^-$  and is shifted to larger distances.

A possible remedy for simple ions would be to employ the “self-consistent” 3D-RISM (SC-3D-RISM) theory.<sup>36</sup> In this approach, one molecule of solvent is labeled and considered as a solute at infinite dilution in the solvent comprising all the other solvent molecules as well as the ionic species present in the solution (at a given concentration which can also be infinite dilution in the case of a single ion). The 3D direct and total correlations of interaction sites of “solvent” species (now including both solvent molecules and ions) around the entire labeled molecule of solvent are obtained from the 3D-RISM theory [eq 2 for the corresponding “solvent” mixture, with some closure, for example, eq 3]. It requires an input of the radial total correlation functions  $h_{\gamma\alpha}^{\text{vv}}(r)$  between interaction sites of pure solvent, including the ion–solvent site correlations. The latter are calculated self-consistently by numerical orientational averaging of the 3D total correlations between the “solute” molecule and the solvent ion obtained from the 3D-RISM equations and then inserted as an input into the 3D-RISM equations in a self-consistent loop. The SC-3D-RISM thus describes the correlations between the solvent molecule and the ion at the 3D level, explicitly incorporating 3-body correlations between the ion and the interaction sites on the same solvent molecule due to its intramolecular bonds.

In both the RISM theory and MD simulations, the peak heights of  $g(r)$  for all solutes are predicted to increase on the transfer from water to water–urea. This is mainly because the density of water in the water–urea mixture is less than that in pure water. It is found that the addition of urea does not change the peak positions of hydration structures around each solute, suggesting that urea molecules can easily penetrate the water liquid structure without a large disruption, as has been pointed out in several theoretical studies<sup>37–41</sup> and experiments.<sup>42–44</sup>

The running coordination numbers  $N$  of the urea carbon site around the  $\text{Cl}^{(0,+,-)}$  solutes, obtained by MD simulations and RISM theory are shown in Figure 2A and B, respectively. The running coordination number  $N_\alpha(\lambda)$ , giving the number of solvent sites  $\alpha$  inside a sphere of radius  $\lambda$  centered at the simple solute, is calculated from the radial distribution function of solvent

$$N_\alpha(\lambda) = \rho_\alpha \int_0^\lambda \text{d}\mathbf{r} g_\alpha(r) \quad (6)$$

where  $\text{d}\mathbf{r}$  denotes the 3D real space differential. In the OPLS force field<sup>31</sup> the carbon site nearly coincides with the center of mass, and it carries a partial charge of +0.142e. We see from both plots (particularly in the MD results shown in Figure 2A) that urea has a certain preference to the positively charged solute. This observation allows us to assume that the urea favors interaction with electrically positive parts in the amino acid residues of native protein and thus starts a denaturation process.

It is of interest to compare the results we obtain with the SPC/E model to earlier work that employed the TIP4P water model.<sup>20</sup> The RDFs obtained for both models by MD simulation are shown in Figure 3. The RDFs for  $\text{Cl}^{(0,+,-)}$  and water (the oxygen) in both pure water and in the water–urea mixture are shown in Figure 3A and B, respectively. In the TIP4P case, the RDFs are between the solute and the auxiliary site (Q site) that carries the negative charge. From these plots we see that the hydration structure in the water–urea mixture is much like that in pure water, and is not sensitive to which of the water models is employed. The distribution of urea (the carbon site of urea) about the different solutes is shown in Figure 3C. We note that these distribution functions are also very similar for the SPC/E and TIP4P water models.

**Transfer Free Energies of Simple Ions and Uncharged Species.** Figure 4A shows the solvation free energy of transfer of cations, anions, and uncharged species from water to a

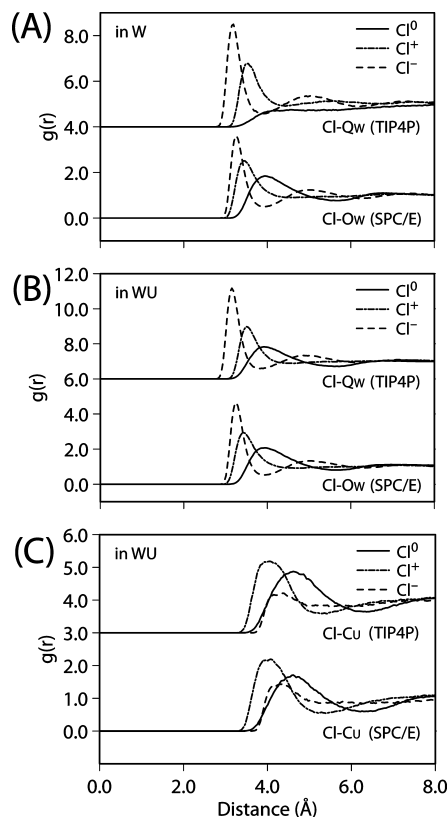


**Figure 3.** RDFs between the chloride-size solutes and solvent molecules obtained by MD simulations. Uncharged, positive, and negative ions are plotted as solid, dash-dotted, and dash lines, respectively. In panel A, RDFs between the solute and the oxygen atom of SPC/E water model and between the solute and the auxiliary site of the TIP4P water model are plotted for pure water. Panel B shows the same RDFs as panel A, but for the water–urea mixture. RDFs between the solute and urea carbon site are presented in panel C. The RDFs for the TIP4P model are displaced upward for clarity.



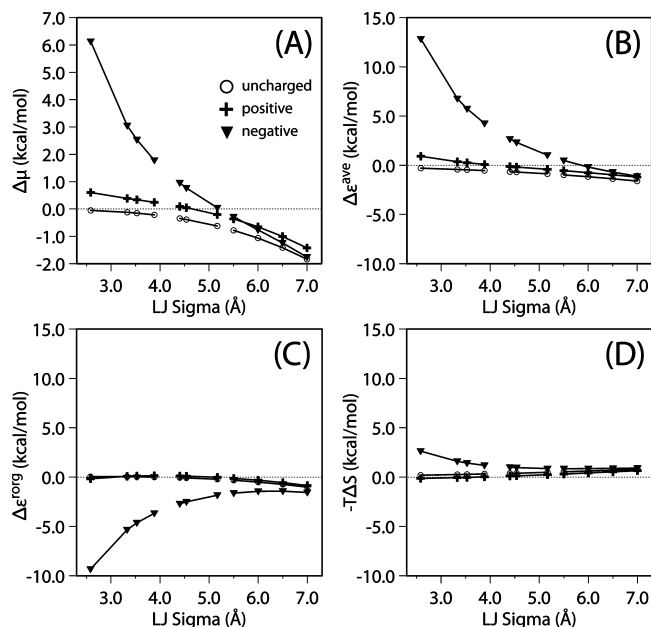


**Figure 4.** Transfer solvation free energy (A) and its components, transfer average solute-solvent energy (B), transfer reorganization energy (C), and transfer solvation entropy (D), are plotted for uncharged solutes (open circles), positive (crosses), and negative ions (lower triangles) as a function of solute diameter (LJ  $\sigma$ ). Order of species in all the plots with increasing LJ  $\sigma$ , respectively: Na, K, Rb, Cs, Cl, Br, I; and four fictitious particles of size 5.5, 6.0, 6.5, and 7.0 Å.

water-urea mixture, which is defined as  $\Delta\mu = \mu_{\text{inWU}} - \mu_{\text{inW}}$ , where  $\mu_{\text{inW}}$  and  $\mu_{\text{inWU}}$  are the solvation free energies in water and in water-urea, respectively. It can be seen from the figure that the transfer of both charged and uncharged species is increasingly favored as the particle size increases and becomes preferred for any species of size above 5.5 Å. This trend is in agreement with experimental<sup>45,46</sup> and theoretical<sup>7,8</sup> results. Comparing the solute-size dependence of the transfer free energy of the ions with that of the corresponding uncharged solutes, we note that the slopes of the ion curves are steeper than those of the uncharged species. This observation implies that the interactions with larger hydrophilic residues might make an important contribution to the stabilization of unfolded protein in water-urea mixture.

To gain further insight, we decompose  $\Delta\mu$  into energetic and entropic parts,  $\Delta\epsilon$  and  $-T\Delta S$ , respectively, based on eq 4.  $\Delta\epsilon$  is further decomposed into the transfer average solute-solvent energy  $\Delta\epsilon^{\text{ave}}$  and the transfer reorganization energy  $\Delta\epsilon^{\text{org}}$ . The decomposition results are shown in Figure 4B, C, and D for  $\Delta\epsilon^{\text{ave}}$ ,  $\Delta\epsilon^{\text{org}}$ , and  $-T\Delta S$ , respectively. From Figure 4 it is evident that the transfer propensity  $\Delta\mu$  as a function of solute size is governed by the quantity  $\Delta\epsilon^{\text{ave}}$ . This analysis suggests that the water-urea mixture stabilizes an unfolded protein through the direct interaction mechanism, as has been proposed by several studies. Recent molecular simulations appear to support the idea that the direct interaction between urea and protein is dominant,<sup>1,3,4</sup> based on analysis of the radial distribution functions. Because  $\Delta\epsilon^{\text{ave}}$  is calculated through the radial distribution function by eq 6, our analysis is consistent with this observation. In effect, the present analysis provides a more robust support for the direct mechanism because our prediction is based on a thermodynamic decomposition in which we compare the effects of the energetic and entropic terms. There have been several investigations in which the entropic contribution is taken into account. These works studied neutral solute species and employed scaled

particle theory<sup>5,6</sup> and molecular simulations.<sup>7,8</sup> These results also suggest that the direct interaction is dominant.

Note that our calculation predicts that the transfer entropy of uncharged species is positive (opposing the transfer), whereas experimental measurement shows it to be negative<sup>45</sup> (preferring the transfer). Possibly, this discrepancy arises because the experimental entropy<sup>45</sup> is obtained under isobaric conditions, whereas we take the derivative of the solvation free energy under the isochoric condition, including the additional contribution from the bulk (see, for example, eq 2.7 in ref 34). Although the experimental transfer entropy of neutral species favors the transfer, it has been shown that the sign of the transfer entropy is determined by the solvent reorganization (alternatively called cavity formation) component of the transfer entropy, that does not contribute to the solvation free energy, and that the solute-solvent van der Waals interaction energy favors the transfer process.<sup>5,6</sup> It is also worth noting that there is a large difference between positively and negatively charged species when the LJ  $\sigma$  is small. This may be related to the theoretical picture that negatively charged species form strong hydrogen bonds with the water hydrogens, with a larger penalty for the disruption of these bonds in the transfer process for the smaller negative solutes.

**Solvation Shell Analysis of Solvation Entropy.** One of the most controversial issues has been the effect of urea on water structure: structure breaker,<sup>47,48</sup> structure maker,<sup>49,50</sup> or negligible changes in the water structure.<sup>4,9,44,51,52</sup> From the present results, we can see that the transfer of a simple solute is not accompanied by a large entropic change. Hence, given the issue mentioned above, it is worth analyzing the reason why the entropic change is not as large in the present transfer process.

We investigate in detail  $-T\Delta S$  by means of a solvation shell analysis. In this analysis, a thermodynamic property is obtained as a function of the distance between the solute and solvent molecules, or as a local property in the subspaces around a solute molecule. Several studies that investigate thermodynamic properties in subspaces around a solute molecule have been reported.<sup>53-58</sup> For instance, Matubayashi et al.<sup>59,60</sup> have introduced the hydration shell model to analyze thermodynamic properties using Monte Carlo simulation. This concept has been extended very recently to 3D molecular theory of solvation (3D-RISM).<sup>61</sup>

In the present analysis, we evaluate the solvation entropy as a function of the distance between the solute and the solvent

$$-TS(\lambda) = \mu(\lambda) - \epsilon(\lambda) \quad (7)$$

where

$$\mu(\lambda) = k_{\text{B}}T \sum_{\text{v}} \sum_{\alpha}^{\text{on v}} \rho_{\alpha} \int_0^{\lambda} \text{d}\mathbf{r} \left[ \frac{1}{2} h_{\alpha}^2(r) \Theta(-h_{\alpha}(r)) - c_{\alpha}(r) - \frac{1}{2} h_{\alpha}(r) c_{\alpha}(r) \right] \quad (8)$$

$$\epsilon(\lambda) = -k_{\text{B}}T \sum_{\text{v}} \sum_{\alpha}^{\text{on v}} \rho_{\alpha} \int_0^{\lambda} \text{d}\mathbf{r} \left[ h_{\alpha}(r) \delta_T h_{\alpha}(r) \Theta(-h_{\alpha}(r)) - \delta_T c_{\alpha}(r) - \frac{1}{2} c_{\alpha}(r) \delta_T h_{\alpha}(r) - \frac{1}{2} h_{\alpha}(r) \delta_T c_{\alpha}(r) \right] \quad (9)$$

The local thermodynamic quantity is defined by introducing a cutoff at distance  $\lambda$ . In eq 9,  $\delta_T$  indicates  $T(\partial/\partial T)$ . Figure 5 shows the solvation shell analysis of  $-TS$  and  $-T\Delta S$  of the chloride-size solute (with charges of 0, +1, and -1) as a function of the cutoff distance.  $-TS_{\text{inW}}$  (blue line) and  $-TS_{\text{inWU}}$  (orange line) indicate the solvation entropies of the solute in water and in the water-urea mixture, respectively.  $-T\Delta S$  is

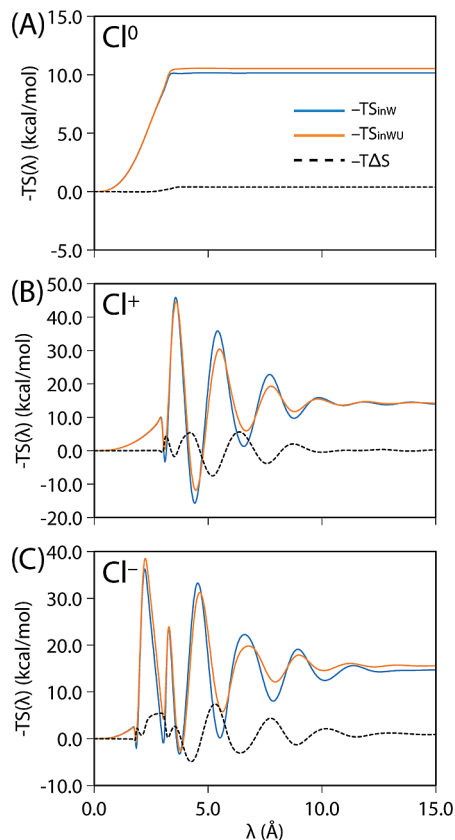


**Figure 5.** Solvation shell analysis of the solvation entropy in water (blue line) and in water–urea (orange line), and their difference (solvation entropy of transfer, black dashed line). Uncharged solute (A), and positive (B) and negative (C) ions.

plotted as a black dashed line. In the present case, it appears that the solvation entropy in the vicinity of the solute (up to about 4 Å) in the water–urea mixture is slightly larger (more structured) than in pure water. However, overall we observe very similar functional behavior in  $-TS_{inW}$  and  $-TS_{inWU}$ , suggesting that, from the viewpoint of solvation entropy, the addition of urea does not change the solvation structure very much. As a result, the entropic contribution to the transfer process is very small.

Next, in order to compare the water–urea mixture to pure water and analyze the solvation entropy in more detail, we regard pure water as a two-component system. In pure water, we define “components” W1 and W2, the former with the number density  $0.02131 \text{ Å}^{-3}$  equal to that of water in the water–urea mixture, and the latter with the complementary number density  $0.01202 \text{ Å}^{-3}$ . In this way, we can see how the hydration changes on transfer by comparing component W1 in pure water ( $-TS_{inW}^{W1}$ ) with the water component in the water–urea mixture ( $-TS_{inWU}^{W1}$ ), and how the hydration by component W2 in pure water ( $-TS_{inW}^{W2}$ ) is altered by the addition of urea in the water–urea mixture ( $-TS_{inWU}^{W2}$ ). Figure 6 presents the decomposition results to compare,  $-TS_{inW}^{W1}$  (blue line) and  $-TS_{inWU}^{W1}$  (orange line). The difference between them is plotted as a black dashed line. Figure 6A, B, and C show the plots for the uncharged, positively charged, and negatively charged solutes, respectively. Figure 7 is the same plot as in Figure 6 but comparing  $-TS_{inW}^{W2}$  (blue line) and  $-TS_{inWU}^{W2}$  (orange line).

From the solvation entropy in the vicinity of solute shown in Figure 6, we see that the peak of  $-TS_{inWU}^{W1}$  is higher than that of  $-TS_{inW}^{W1}$  for all cases, suggesting that the hydration structure around the solute in the water–urea mixture is more rigid than

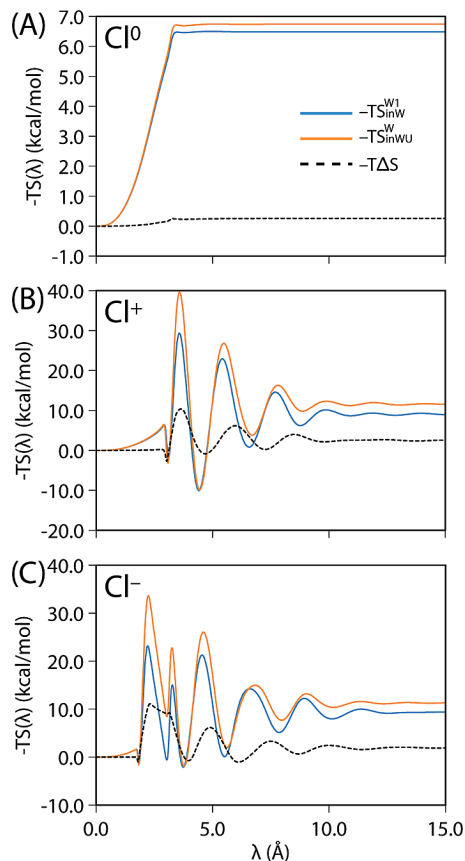


**Figure 6.** Solvation shell analysis of the solvation entropy of W1 in water (blue line), W1 in water–urea (orange line), and their difference (black dashed line) for uncharged solute (A), and positive (B) and negative (C) ions. W1 is the component of pure water that has the same density as water (denoted as W) in the water–urea mixture.

in pure water. This may be a manifestation of the urea’s ability as a structure maker, consistent with the rotational motion of water molecules in a water–urea mixture observed by NMR spectroscopy.<sup>62</sup> The view of urea strengthening water structure and making it more “ice-like” has also been suggested by recent molecular dynamics simulation.<sup>41</sup> On the other hand, the peak of  $-TS_{inWU}^{W1}$  is lower than that of  $-TS_{inW}^{W2}$ , as shown in Figure 7. We can consider that this is because the liquid structure of urea is less ordered than the hydrogen-bond network of water. Due to these two effects compensating each other, a large entropic change does not show up in the transfer process. In the case of a chloride-size solute, the former effect dominates the latter. As a result, the transfer solvation entropy in the vicinity of the solute becomes positive, as seen in Figure 5. However, we should not draw a final conclusion at this point, as to whether or not urea is a structure maker, because we have only seen the solvation picture from the point of view of the solute molecule and not from that of solvent. To further uncover this longstanding issue, we would need to investigate the solvent–solvent correlation in the presence of a solute molecule, which would require an inhomogeneous liquid state theory such as the inhomogeneous reference interaction site model (inhomogeneous RISM) theory recently developed by Ishizuka et al.<sup>63</sup> In the present article, we limit ourselves to the statement that the existence of these two effects compensating each other may be one reason for the existence of the uncertainty about the urea effect on the water structure.

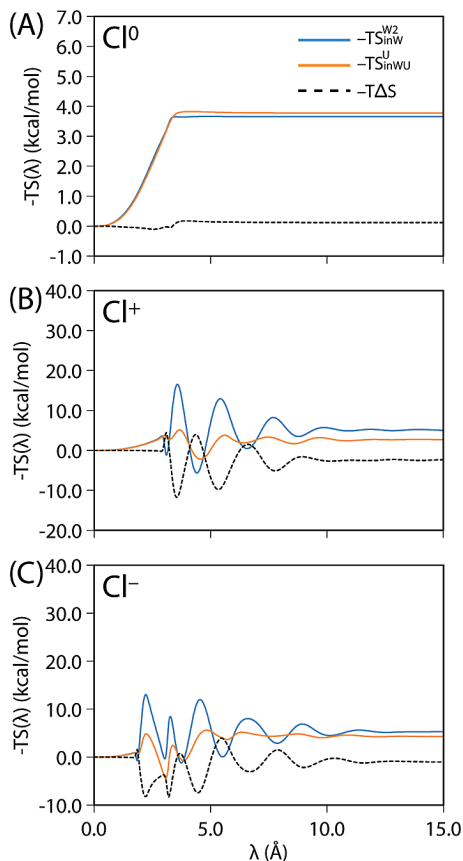


**Figure 7.** Solvation shell analysis of the solvation entropy of W2 in water (blue line), U in water–urea (orange line), and their difference (black dash line) for uncharged solute (A), and positive (B) and negative (C) ions. W2 is the component of pure water and has the complementary number density of W1 for pure water. U is the urea component in water–urea mixture.

### Concluding Remarks

In this paper we have employed MD simulations and molecular theory of solvation (RISM) to obtain the solvation structure of solutes in a water–urea mixture. We have considered positive and negative ions as well as uncharged species, which can be viewed as simplified models for the hydrophilic and hydrophobic groups of a protein. The solute–solvent distribution functions obtained indicate that, whereas urea has a preference for positively charged solutes, it does not disrupt significantly the hydration shell of water around any solute considered. Using the RISM theory, we have calculated the solvation free energy of transfer from water to the water–urea mixture. Our results are in agreement with experiment, in that the transfer is favorable for larger solutes, both in the charged and uncharged cases. We have also analyzed the transfer free energy by decomposing it into the energetic and entropic terms. This analysis clearly shows that the entropic contribution is relatively small, and the transfer process is dominated by energetic considerations. From the solvation shell analysis of solvation entropy, we found that the water molecules in the water–urea mixture are a bit more structured than pure water, whereas the urea molecules in the water–urea mixture are less structured, in terms of the solvation entropy, than pure water. We suggested that the existence of these two components compensating each other may be one of the reasons for the uncertainty concerning the effect of urea on water structure and biomolecular hydration.

**Acknowledgment.** We gratefully acknowledge the financial support of the National Research Council of Canada (T.Y. and A.K.) and of the Natural Science and Engineering Research Council of Canada (V.V.M. and G.N.P.). A.K. thanks the Department of Chemistry, University of British Columbia, for the hospitality during his stay there. This research has been enabled by the use of WestGrid computing resources, which are funded in part by the Canada Foundation for Innovation, Alberta Innovation and Science, BC Advanced Education, and the participating research institutions. WestGrid equipment is provided by IBM, Hewlett-Packard, and SGI. The computations were also supported by the Centre of Excellence in Integrated Nanotools (CEIN) at the University of Alberta.

**Supporting Information Available:** Transfer free energy of the aliphatic hydrocarbons and simple ions from water to water–urea mixture calculated by several closure relations and theoretical details of those closure relations. This material is available free of charge via the Internet at <http://pubs.acs.org>.

### References and Notes

- (1) Wallqvist, A.; Covell, D. G.; Thirumalai, D. *J. Am. Chem. Soc.* **1998**, *120*, 427–428.
- (2) Ikeguchi, M.; Nakamura, S.; Shimizu, K. *J. Am. Chem. Soc.* **2001**, *123*, 677–682.
- (3) Tobi, D.; Elber, R.; Thirumalai, D. *Biopolymers* **2003**, *68*, 359–369.
- (4) Mountain, R. D.; Thirumalai, D. *J. Am. Chem. Soc.* **2003**, *125*, 1950–1957.
- (5) Graziano, G. *J. Phys. Chem. B* **2001**, *105*, 2632–2637.
- (6) Graziano, G. *Can. J. Chem.* **2002**, *80*, 388–400.
- (7) van der Vegt, N. F. A.; Trzesniak, D.; Kasumaj, B.; van Gunsteren, W. F. *ChemPhysChem* **2004**, *5*, 144–147.
- (8) Trzesniak, D.; van der Vegt, N. F. A.; van Gunsteren, W. F. *Phys. Chem. Chem. Phys.* **2004**, *6*, 697–702.
- (9) Klimov, D. K.; Straub, J. E.; Thirumalai, D. *Proc. Natl. Acad. Sci. USA* **2004**, *101*, 14760–14765.
- (10) Caballero-Herrera, A.; Nordstrand, K.; Berndt, K. D.; Nilsson, L. *Biophys. J.* **2005**, *89*, 842–857.
- (11) Oostenbrink, C.; van Gunsteren, W. F. *Phys. Chem. Chem. Phys.* **2005**, *7*, 53–58.
- (12) Lee, M.-E.; van der Vegt, N. F. A. *J. Am. Chem. Soc.* **2006**, *128*, 4948–4949.
- (13) O'Brien, E. P.; Dima, R. I.; Brooks, B.; Thirumalai, D. *J. Am. Chem. Soc.* **2007**, *129*, 7346–7353.
- (14) Bennion, B. J.; Daggett, V. *Proc. Natl. Acad. Sci. USA* **2003**, *100*, 5142–5147.
- (15) Stumpe, M. C.; Grubmüller, H. *J. Am. Chem. Soc.* **2007**, *129*, 16126–16131.
- (16) Hirata, F.; Rossky, P. J. *J. Chem. Phys. Lett.* **1981**, *83*, 329–334.
- (17) Hirata, F.; Pettitt, B. M.; Rossky, P. J. *J. Chem. Phys.* **1982**, *77*, 509–520.
- (18) Hirata, F.; Rossky, P. J.; Pettitt, B. M. *J. Chem. Phys.* **1983**, *78*, 4133–4144.
- (19) *Molecular Theory of Solvation*; Hirata, F., Ed.; Kluwer Academic Publishers: Dordrecht, The Netherlands, 2003; Vol. 24.
- (20) Duffy, E. M.; Kowalczyk, P. J.; Jorgensen, W. L. *J. Am. Chem. Soc.* **1993**, *115*, 9271–9275.
- (21) Hefter, G.; Marcus, Y.; Waghorne, W. E. *Chem. Rev.* **2002**, *102*, 2773–2836.
- (22) Kovalenko, A.; Hirata, F. *J. Chem. Phys.* **1999**, *110*, 10095–10112.
- (23) Kovalenko, A.; Hirata, F. *J. Chem. Phys. Lett.* **2001**, *349*, 496–502.
- (24) Chandler, D.; Singh, Y.; Richardson, D. M. *J. Chem. Phys.* **1984**, *81*, 1975–1982.
- (25) Ichiye, T.; Chandler, D. *J. Phys. Chem.* **1988**, *92*, 5257–5261.
- (26) Yu, H.-A.; Pettitt, B. M.; Karplus, M. *J. Am. Chem. Soc.* **1991**, *113*, 2425–2434.
- (27) Lee, P. H.; Maggiora, G. M. *J. Phys. Chem.* **1993**, *97*, 10175–10185.
- (28) Sato, K.; Chuman, H.; Ten-no, S. *J. Phys. Chem. B* **2005**, *109*, 17290–17295.
- (29) Berendsen, H. J. C.; Grigera, J. R.; Straatsma, T. P. *J. Phys. Chem.* **1987**, *91*, 6269–6271.
- (30) Pettitt, B. M.; Rossky, P. J. *J. Chem. Phys.* **1982**, *77*, 1451–1457.
- (31) Duffy, E. M.; Severance, D. L.; Jorgensen, W. L. *Isr. J. Chem.* **1993**, *33*, 323–330.

- (32) Koneshan, S.; Rasaiah, J. C.; Lynden-Bell, R. M.; Lee, S. H. *J. Phys. Chem. B* **1998**, *102*, 4193–4204.
- (33) Ishida, T.; Rossky, P. J.; Castner, E. W., Jr. *J. Phys. Chem. B* **2004**, *108*, 17583–17590.
- (34) Yu, H.-A.; Roux, B.; Karplus, M. *J. Chem. Phys.* **1990**, *92*, 5020–5033.
- (35) Allen, M. P.; Tildesley, D. J. *Computer Simulation of Liquids*; Clarendon Press: New York, NY, USA, 1989.
- (36) Kovalenko, A.; Truong, T. N. *J. Chem. Phys.* **2000**, *113*, 7458–7470.
- (37) Tanaka, H.; Touhara, H.; Nakanishi, K.; Watanabe, N. *J. Chem. Phys.* **1984**, *80*, 5170–5186.
- (38) Kuharski, R. A.; Rossky, P. J. *J. Am. Chem. Soc.* **1984**, *106*, 5786–5793.
- (39) Åstrand, P.-O.; Wallqvist, A.; Karlström, G.; Linse, P. *J. Chem. Phys.* **1991**, *95*, 8419–8429.
- (40) Kokubo, H.; Pettitt, B. M. *J. Phys. Chem. B* **2007**, *111*, 5233–5242.
- (41) Stumpe, M. C.; Grubmüller, H. *J. Phys. Chem. B* **2007**, *111*, 6220–6228.
- (42) Finney, J. L.; Soper, A. K.; Turner, J. *Physica B* **1989**, *156–157*, 151–153.
- (43) Sharp, K. A.; Madan, B.; Manas, E.; Vanderkooi, J. M. *J. Chem. Phys.* **2001**, *114*, 1791–1796.
- (44) Grdadolnik, J.; Maréchal, Y. *J. Mol. Struct.* **2002**, *615*, 177–189.
- (45) Wetlaufer, D. B.; Malik, S. K.; Stoller, L.; Coffin, R. L. *J. Am. Chem. Soc.* **1964**, *86*, 508–514.
- (46) Nandi, P. K.; Robinson, D. R. *Biochemistry* **1984**, *23*, 6661–6668.
- (47) Finer, E. G.; Franks, F.; Tait, M. J. *J. Am. Chem. Soc.* **1972**, *94*, 4424–4429.
- (48) Hoccart, X.; Turrell, G. *J. Chem. Phys.* **1993**, *99*, 8498–8503.
- (49) Vanzi, F.; Madan, B.; Sharp, K. *J. Am. Chem. Soc.* **1998**, *120*, 10748–10753.
- (50) Chitra, R.; Smith, P. E. *J. Phys. Chem. B* **2000**, *104*, 5854–5864.
- (51) Åstrand, P.-O.; Wallqvist, A.; Karlström, G. *J. Phys. Chem.* **1994**, *98*, 8224–8233.
- (52) Tirado-Rives, J.; Orozco, M.; Jorgensen, W. L. *Biochemistry* **1997**, *36*, 7313–7329.
- (53) Mehrotra, P. K.; Beveridge, D. L. *J. Am. Chem. Soc.* **1980**, *102*, 4287–4294.
- (54) Mezei, M.; Beveridge, D. L. *Methods Enzymol.* **1986**, *127*, 21–47.
- (55) Levitt, M.; Sharon, R. *Proc. Natl. Acad. Sci. USA* **1988**, *85*, 7557–7561.
- (56) Lounnas, V.; Pettitt, B. M. *Proteins: Struct. Funct. Bioinf.* **1994**, *18*, 133–147.
- (57) Ashbaugh, H. S.; Paulaitis, M. E. *J. Phys. Chem.* **1996**, *100*, 1900–1913.
- (58) Ashbaugh, H. S.; Paulaitis, M. E. *J. Am. Chem. Soc.* **2001**, *123*, 10721–10728.
- (59) Matubayasi, N.; Reed, L. H.; Levy, R. M. *J. Phys. Chem.* **1994**, *98*, 10640–10649.
- (60) Matubayasi, N.; Levy, R. M. *J. Phys. Chem.* **1996**, *100*, 2681–2688.
- (61) Yamazaki, T.; Kovalenko, A. *J. Chem. Theory Comput.* **2009**, *5*, 1723–1730.
- (62) Yoshida, K.; Ibuki, K.; Ueno, M. *J. Chem. Phys.* **1998**, *108*, 1360–1367.
- (63) Ishizuka, R.; Chong, S.-H.; Hirata, F. *J. Chem. Phys.* **2008**, *128*, 034504.

JP908814T